Band to band tunneling in heterojunctions: Semi-classical versus quantum computation

Arvind Ajoy
Department of Electrical Engineering
Indian Institute of Technology Madras
Chennai 600036, India
arvindajoy@iitm.ac.in

***Abstract*—Band-to-band tunneling (BTBT) determines the on-current in tunnel FETs (TFETs). There is a need to review and recalibrate BTBT models used in TCAD tools, which were developed when BTBT was essentially a leakage phenomenon. Here, we consider the process of BTBT through staggered heterojunctions which find application in the design of TFETs having high on-currents. We use a simple 1-D system and compare the estimates of BTBT computed with a semi-classical WKB approach and that obtained from a solution of Schrödinger's equation by a wavefunction matching procedure. We show that the WKB method significantly overestimates the tunneling current through heterojunctions.**

***Index Terms*—Band-to-band tunneling, heterojunctions, complex bandstructure, WKB, NEGF.**

I. Introduction

Accurate and computationally efficient approaches to simulate band-to-band tunneling (BTBT) are required to optimize the performance of modern semiconductor devices. In particular, the design of Tunnel FETs (TFETs) requires very reliable BTBT simulation models, since BTBT is responsible for I_{on} in TFETs, whereas it only determines leakage currents in MOSFETs. TFETs can operate at lower supply voltages than conventional MOSFETs, owing to their superior ($< 60\ mV/dec$) sub-threshold slope, and are hence attractive for low power applications. However, it is difficult to achieve reasonable on-currents ($I_{on} > 100\ \mu A/\mu m$) in these devices. Nevertheless, an appropriately designed heterojunction (see Fig. 1) can achieve MOSFET-like I_{on} in TFETs [1]. From this point of view, TCAD tools must be able to reliably handle BTBT through heterojunctions.

It is known that a multiscale approach which captures the complex bandstructure within the bandgap of the semiconductor is critical to reliably predict BTBT current through homojunctions [2], [3]. Evanescent states in heterojunctions depend on both materials forming the junction. However, semi-classical schemes to handle BTBT through heterojunctions (e.g. [4]) simply follow a region based approach, stitching together the complex bands of the two materials. The accuracy of computing BTBT current using this idea is not known. In this work, we compare this semi-classical approach against the results of an accurate quantum approach, using a simple 1-D system.

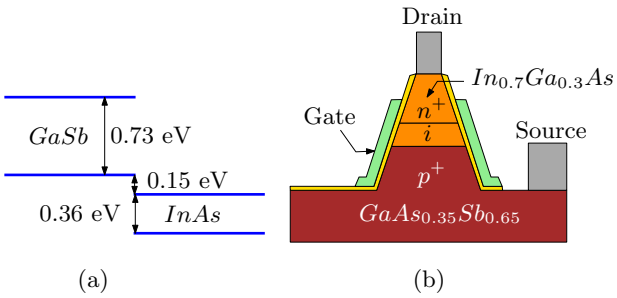

Fig. 1. (a) Broken-gap band alignment in GaSb/InAs (from Ref. [7]). (b) Schematic cross section of an N-TFET [1] with MOSFET-like on-current, $I_{on} = 190\ \mu A/\mu m$. Based on strain and composition, the alignment at the p^+-i junction could be broken or staggered.

II. Procedure

A. Model system

Our model system is a p-n junction formed in a linear chain of atoms described by a simple two-band second-nearest neighbor tight binding model [5], [6]. A real p-n junction can be regarded as a parallel stacking of such chains. This model places a p_x orbital on an anion and an s-orbital on a cation as shown in Fig. 2 and is known to capture the essential features of the bandstructure of direct bandgap materials. There are five parameters in this model – the on-site energies for the s and p_x orbitals (E_s, E_p), the nearest neighbor overlap of an s and p_x orbital (V_{sp}), and the second-nearest neighbor overlap of two s and p_x orbitals (V_s, V_p). These parameters have to be obtained from the position of the valence (E_v) and conduction (E_c) band edges and their corresponding effective masses m_v, m_c (both defined to be positive and in units of the free electron mass m_0). We restrict ourselves to the case where $m_v \neq m_c$, so that we can choose $V_s = V_p = V_0$. Defining $\eta = (m_c + m_v)/(m_c - m_v)$ and $C = \hbar^2/m_0 a^2$, where a is the lattice constant, we obtain

$$V_0 = \frac{2C}{m_c}\frac{1}{\eta - 1} \tag{1a}$$

$$V_{sp} = +\sqrt{\eta V_0\,(E_c - E_v)} \tag{1b}$$

$$E_s = E_c - 2V_0 \tag{1c}$$

$$E_p = E_v - 2V_0 \tag{1d}$$

We now consider two direct bandgap materials A and B with

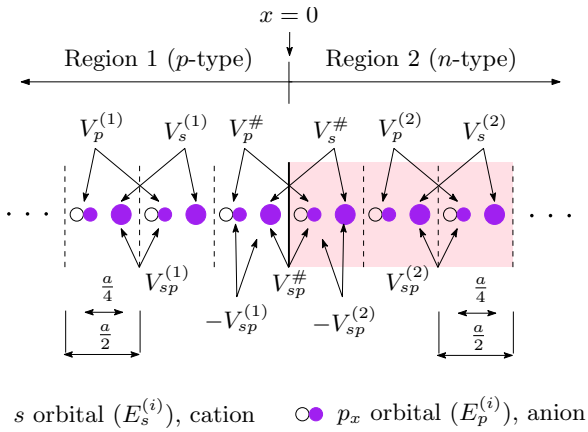

Fig. 2. A p-n junction formed using a linear chain of atoms, showing interatomic tight binding matrix elements [5]. $V_x^{\#} = (V_x^{(1)} + V_x^{(2)})/2$. On-site elements are $E_s^{(i)}, E_p^{(i)}$ $(i = 1, 2)$ for the s and p_x orbitals located in regions 1 and 2 respectively. The positive lobe of each orbital has been shown shaded.

a staggered (Type-II) band alignment as shown in Fig. 3(a). Such an alignment provides a small effective bandgap $E_{g,eff}$ for tunneling and is of interest in TFET design. Following [6], the tight binding matrix elements at the interface at $x = 0$ are written as an average of those in the materials on both sides of the interface. We assume the electrostatic potential under applied bias to be the same as that in a real p-n junction (with doping concentrations N_{A_1}, N_{D_2} in regions 1, 2) under a depletion approximation; the doping concentrations are chosen so as to align the Fermi levels on the p and n sides of the junction to the corresponding valence and conduction band edges. Ignoring Fermi statistics, we thus obtain the built-in potential w.r.t region 1, V_{bi} as

$$V_{bi} = \frac{\Delta E_c - \Delta E_v}{2} - V_t \ln\left(\frac{n_{i_1} n_{i_2}}{N_{A_1} N_{D_2}}\right) \tag{2}$$

where $\Delta E_c = E_{c_2} - E_{c_1}$, $\Delta E_v = E_{v_1} - E_{v_2}$ and n_i, V_t are the intrinsic carrier concentration and thermal voltage respectively.

B. Computation of tunneling current

The complex bandstructures of materials A and B are computed using a generalized eigenvalue method [8] and are shown in Fig. 3(b).

The BTBT tunneling current is written as

$$I = \frac{2q}{h} \int T(E)\,(f_1(E) - f_2(E))\,dE \tag{3}$$

where $T(E)$ is the transmission and $f_1(E)$, $f_2(E)$ are the Fermi levels in regions 1, 2 respectively. An accurate computation of $T(E)$ is performed using the wavefunction matching method [9]. This is equivalent to the Non Equilibrium Green's Function (NEGF) method for the case of coherent transport, but is simpler to implement and computationally more efficient. A summary of the wavefunction matching algorithm is presented in the Appendix. A semi-classical estimate using a

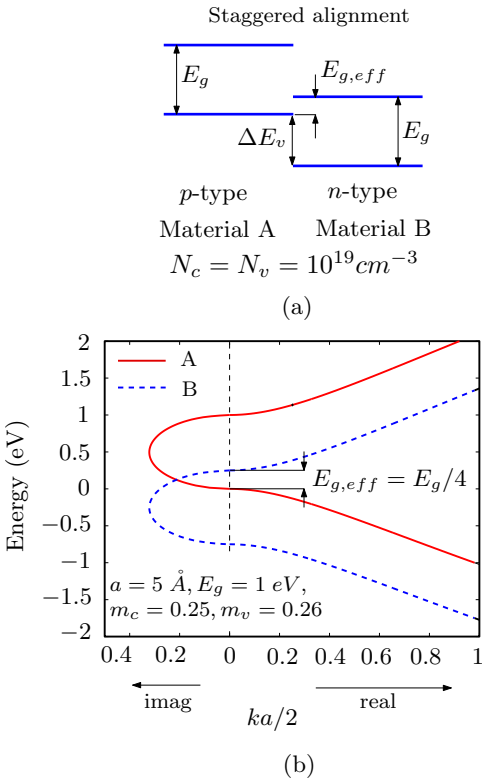

Fig. 3. (a) Band alignment between materials A and B considered in this work. These materials differ only in their electron affinities. $E_{g,eff}$ is the effective bandgap for band-to-band tunneling if material A is p-type and B is n-type. N_c and N_v are the effective density of states in the conduction and valence bands. (b) Real and imaginary energy bands of material A (solid) and material B (dashed).

WKB approximation [10] for $T(E)$ is given by

$$T(E) = -2\Big[\int_{x_1}^{0} \kappa_1(E - E_v(x))dx + \int_{0}^{x_2} \kappa_2(E - E_v(x) - \Delta E_v)dx\Big] \tag{4}$$

where x_1, x_2 are the classical turning points and κ_1, κ_2 are

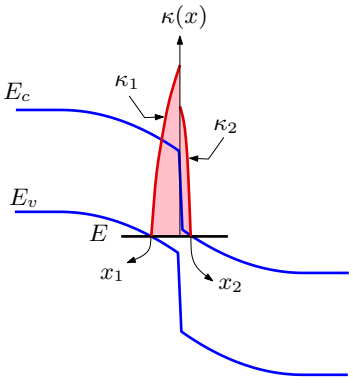

Fig. 4. Stitching of imaginary wavevectors across a heterointerface following Ref. [4]. x_1, x_2 are the classical turning points at the energy E. The imaginary wavevectors κ_1, κ_2 are obtained from the complex bandstructures of materials in regions 1, 2 respectively.

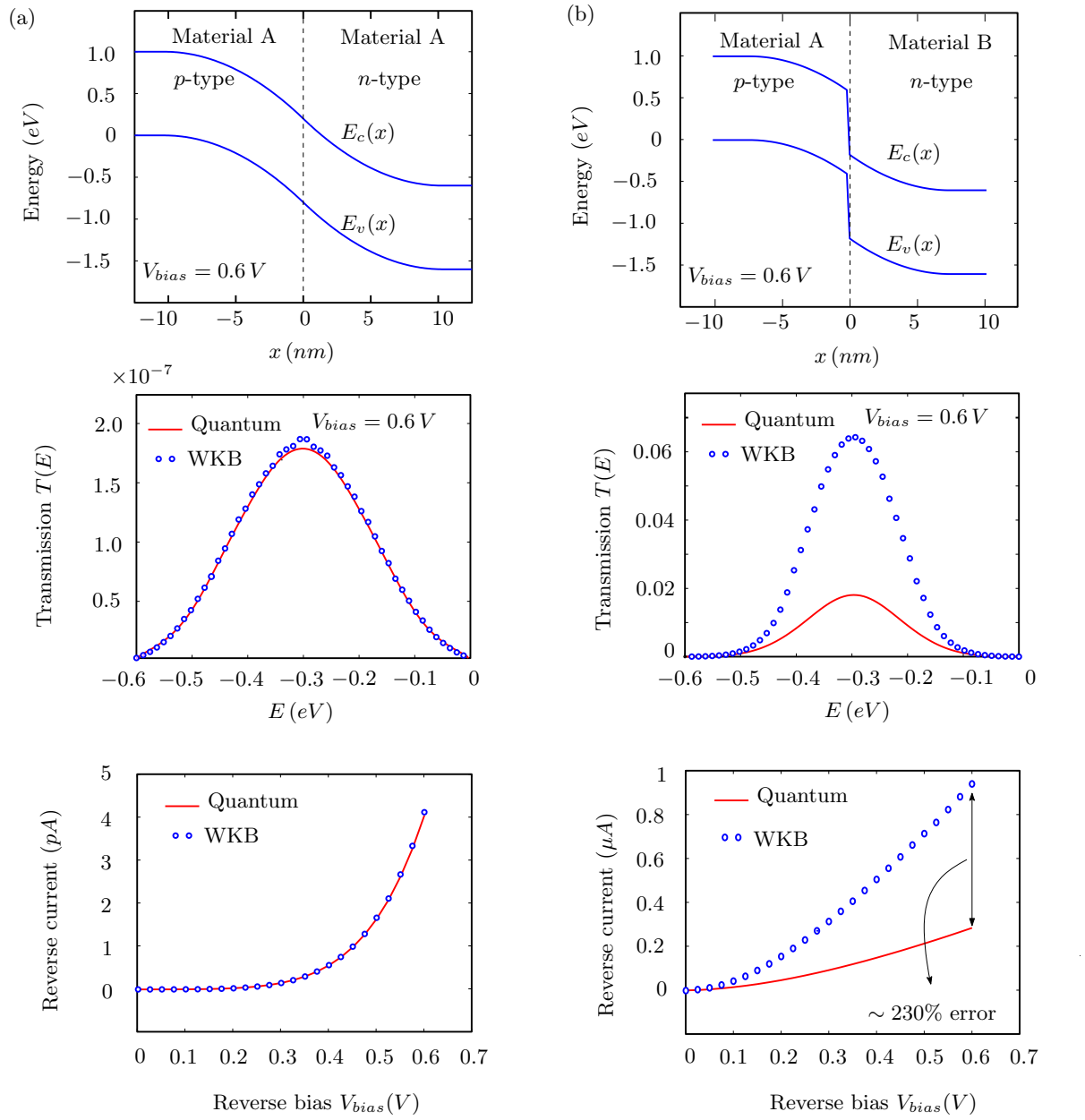

Fig. 5. Comparison of transmission $T(E)$ and current calculated using quantum and semi-classical approaches in an (a) A-A homojunction and (b) A-B heterojunction. The Fermi levels are assumed to coincide with the valence and conduction band edges on the p and n sides respectively.

the imaginary wavevectors in regions 1, 2. These are obtained from the complex bandstructure shown in Fig. 3(b). Note that we do not attempt to solve the transport problem self-consistently with the electrostatics. Nevertheless, this is not critical to our results, since we use the same potential landscape to compute $T(E)$ semi-classically and via the wavefunction matching technique.

III. Results and Conclusion

See Fig. 5. The semi-classical WKB approach compares very well with the quantum calculation for the case of a homojunction in a direct bandgap material. This is consistent with a result available in literature [10], which demonstrates that the semi-classical WKB approach provides a good estimate for $T(E)$ in materials where a single imaginary band connecting the real valence and conduction bands is the dominant tunneling path.

On the other hand, the WKB approach significantly overestimates the current in the heterojunction. This could be due to the discontinuity in the imaginary wavevector $\kappa(x)$ at the heterointerface, obtained by stitching the wavevectors on either side of the interface (as seen, for example, in Fig. 4). A transfer matrix based approach might hence yield better results. We also believe that the stitching of imaginary wavevectors must include a correction based on the connection rules for the envelope functions across the heterojunction [11]. This will

be taken up in a future work.

Since a quantum calculation of $T(E)$ is computationally demanding for realistic devices, our study motivates the need for better semi-classical approaches to handle BTBT through heterojunctions. Further, our procedure can be used to study this problem in other types of band alignments too.

APPENDIX
SUMMARY OF WAVEFUNCTION MATCHING

In this appendix, we summarize the steps involved in the wavefunction matching procedure [9]. The system under study is separated into a "device" region and "leads", as shown in Fig. 6.

1) Each of the matrices in Fig. 6 is of size $N \times N$. Obtain the N forward $(+)$ and N backward $(-)$ modes $[u_{L/R,n}(\pm)]$, $n = 1, 2, \ldots N$ in each lead L/R, as the eigenvectors of the generalized eigenvalue problem

$$-[B_{L/R}][c_{i-1}] + (E[I] - [H_{L/R}])[c_i] - [B_{L/R}]^\dagger[c_{i+1}] = [0],$$

where $[c_{i+1}] = \lambda_n(\pm)[c_i]$. These modes have velocities given by

$$v_{L/R,n}(\pm) = -\frac{a_{L/R}}{\hbar} \times \mathrm{Im}(\lambda_n(\pm)[u_{L/R,n}(\pm)]^\dagger[B_{L/R}]^\dagger[u_{L/R,n}(\pm)]).$$

2) Compute the dual vectors $[\tilde{u}_{L/R,n}(\pm)]$ and Bloch matrices $[F_{L/R}(\pm)]$ defined as

$$[\tilde{u}^\dagger_{L/R,n}(\pm)][u_{L/R,m}(\pm)] = \delta_{n,m}$$
$$[F_{L/R}(\pm)] = \sum_{n=1}^{N} \lambda_n(\pm)[u_{L/R,n}(\pm)][\tilde{u}_{L/R,n}(\pm)]^\dagger$$

3) Construct the self energies $[\Sigma_L(E)] = [B_L][F_L^{-1}(-)]$ and $[\Sigma_R(E)] = [B_R]^\dagger[F_R(+)]$.

4) Construct the auxiliary matrix $[\mathcal{H}]$ of size $N(S+2) \times N(S+2)$, such that the block $[\mathcal{H}_{i,j}] = [H_{i,j}]$ for $i, j = 0, \ldots, S+1$ except for

$$[\mathcal{H}_{0,0}] = [H_L] + [\Sigma_L]$$
$$[\mathcal{H}_{S+1,S+1}] = [H_R] + [\Sigma_R].$$

5) Construct and solve the system of linear equations given by $(E[I] - [\mathcal{H}])\,[\psi] = [Q_{L,m}(+)]$, where

$$[\psi] = [\,[c_0],\ \ldots,\ [c_{S+1}]\,]^T$$
$$[Q_{L,m}(+)] = \begin{bmatrix} [X] \\ [0] \\ \vdots \\ [0] \end{bmatrix} \text{ and}$$
$$[X] = [B_L]\left([F_L(+)]^{-1} - [F_L(-)]^{-1}\right)[u_{L,m}(+)].$$

6) Finally, the transmission

$$T(E) = \sum_{n,m}^{(+)} |t_{n,m}|^2,$$

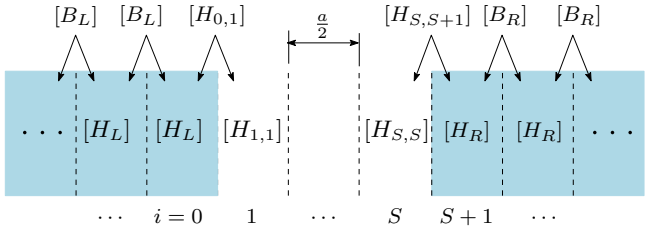

Fig. 6. Matrices involved in the wavefunction matching procedure [9]. The potential is assumed to be constant in the leads (shown shaded) but can vary in the device (slabs $1, ..., S$).

where $t_{n,m} = \sqrt{\frac{v_{R,n}(+)a_L}{v_{L,m}(+)a_R}}\tau_{n,m}$ and $\tau_{n,m} = [\tilde{u}_{R,n}(+)][c_{S+1}]$.

ACKNOWLEDGMENT

The author thanks his PhD advisor Prof. Shreepad Karmalkar for channeling his ideas into the form presented in this paper. He also thanks Dr. Kota Murali (IBM SRDC, Bangalore) for useful discussions, and acknowledges financial support from IBM India.

REFERENCES

[1] D. K. Mohata, R. Bijesh, S. Mujumdar, C. Eaton, R. Engel-Herbert, T. Mayer, V. Narayanan, J. M. Fastenau, D. Loubychev, A. K. Liu, and S. Datta, "Demonstration of MOSFET-like on-current performance in arsenide/antimonide tunnel FETs with staggered hetero-junctions for 300mV logic applications," in *2011 IEEE International Electron Devices Meeting (IEDM)*, Dec. 2011, pp. 33.5.1 –33.5.4.

[2] S. Laux, "Computation of Complex Band Structures in Bulk and Confined Structures," in *13th International Workshop on Computational Electronics (IWCE)*. IEEE, 2009, pp. 1–2.

[3] R. Pandey, K. Murali, S. Furkay, P. Oldiges, and E. Nowak, "Crystallographic-Orientation-Dependent Gate-Induced Drain Leakage in Nanoscale MOSFETs," *IEEE Trans. Electron Devices*, vol. 57, no. 9, pp. 2098 –2105, 2010.

[4] A. S. Verhulst, W. G. Vandenberghe, K. Maex, and G. Groeseneken, "Boosting the on-current of a n-channel nanowire tunnel field-effect transistor by source material optimization," *J. Appl. Phys.*, vol. 104, no. 6, p. 064514, 2008.

[5] G. A. Sai-Halasz, L. Esaki, and W. A. Harrison, "InAs-GaSb superlattice energy structure and its semiconductor-semimetal transition," *Phys. Rev. B*, vol. 18, pp. 2812–2818, Sep 1978.

[6] T. Boykin, "Tunneling calculations for systems with singular coupling matrices: results for a simple model," *Phys. Rev. B*, vol. 54, no. 11, p. 7670, 1996.

[7] E. T. Yu, J. O. McCaldin, and T. C. McGill, "Band offsets in semiconductor heterojunctions," ser. Solid State Physics, H. Ehrenreich and D. Turnbull, Eds. Academic Press, 1992, vol. 46, pp. 1 – 146.

[8] T. Boykin, "Generalized eigenproblem method for surface and interface states: the complex bands of GaAs and AlAs," *Phys. Rev. B*, vol. 54, no. 11, pp. 8107–8115, 1996.

[9] P. Khomyakov, G. Brocks, V. Karpan, M. Zwierzycki, and P. Kelly, "Conductance calculations for quantum wires and interfaces: Mode matching and Green's functions," *Phys. Rev. B*, vol. 72, no. 3, p. 035450, 2005.

[10] M. Luisier and G. Klimeck, "Simulation of nanowire tunneling transistors: From the Wentzel–Kramers–Brillouin approximation to full-band phonon-assisted tunneling," *J. Appl. Phys.*, vol. 107, no. 8, p. 084507, 2010.

[11] T. Ando, S. Wakahara, and H. Akera, "Connection of envelope functions at semiconductor heterointerfaces. I. interface matrix calculated in simplest models," *Phys. Rev. B*, vol. 40, no. 17, p. 11609, 1989.